

Dynamics and melting of a thin confined film

O. M. Braun

Institute of Physics, National Academy of Sciences of Ukraine, 03650 Kiev, Ukraine

M. Peyrard

Laboratoire de Physique de l'Ecole Normale Supérieure de Lyon, 46 Allée d'Italie, 69364 Lyon Cédex 07, France

(Received 5 December 2002; published 23 July 2003)

Molecular dynamics is used to investigate the melting of a thin lubricant film confined between two crystalline surfaces. The dynamics of the film is significantly affected by the substrate, both in the solid and in the molten phases. The solid phase, able to sustain shear stress, shows, however, large diffusional motions of the atoms. The melting temperature depends strongly on the confinement. A phenomenological microscopic theory, based on the Lindemann criterion, is proposed to explain this effect.

DOI: 10.1103/PhysRevE.68.011506

PACS number(s): 64.70.Dv, 68.08.-p

I. INTRODUCTION

The properties of fluids confined between crystalline surfaces that are only a few nanometers apart are still far from being understood in spite of many recent studies, using either numerical simulations [1,2] or high precision experiments [3,4]. The unresolved questions concern both the structure of the film and the melting transition between the crystallized phase and the molten phase of the film, which could play a role in the stick slip at the microscopic scale observed in some numerical simulations of friction [1,2].

The various approaches agree that in a liquid film with a width smaller than about 10 molecular diameters, the atoms in the film are ordered into layers that are parallel to the bounding walls [5–10]. When the width of the lubricant film is reduced even further, numerical simulations generally conclude that the film behaves as a solid, even at temperatures significantly higher than its bulk melting temperature [1,2]. However, recent experimental studies have shown that the confinement-induced “solid” does not have a well-defined structure in which molecules are fixed in space [4]. This raises an interesting question because, on one hand, the lubricant appears to be able to sustain a shear stress, and, on the other hand, a large diffusion of the molecules is observed.

Another question that is still open is the thermodynamics of the melting transition in a highly confined environment. Experiments and simulation show that the melting temperature is higher than in the bulk but the quantitative analysis of this phenomenon is still incomplete. A simple approach based on the Lindemann criterion and the confinement of the fluctuations by the walls has been proposed [11]. It provides interesting results but is based on a continuous model of the elasticity of the layer, which becomes questionable when the layer has only a few atomic planes. Another continuum approach uses a Ginzburg-Landau expression and a mean-field theory [12], but no microscopic model of confined melting has been proposed.

Our aim in this work is double. First, we would like to clarify the structure and dynamics of a highly confined atomic fluid using molecular dynamics simulations, and second, we want to investigate its melting transition, with a

simple microscopic model to calculate the dependence of the melting temperature on the film thickness and compare the results with the simulations. Although these studies could be relevant for the microscopic theory of friction, for which the melting and freezing of the lubricant are suspected to play an important role [1,2], we have concentrated our attention on the properties of the confined film as a function of temperature, which are usually not accessible to surface-force apparatus experiments.

II. MODEL

The model is schematized in Fig. 1. It was presented in a previous paper [13] and, therefore, we only briefly discuss here its main features. Using molecular dynamics, we study a few atomic-layer film between two parallel top and bottom substrates. Each substrate is made of two layers. One is fully rigid while the dynamics of the atoms belonging to the layer in contact with the confined fluid is included in the study. The rigid part of the bottom substrate is fixed, while the rigid layer of the top substrate is mobile in the three directions of space x, y, z .

All the atoms interact with the Lennard-Jones potentials

$$V(r) = V_{\alpha\alpha'} \left[\left(\frac{r_{\alpha\alpha'}}{r} \right)^{12} - 2 \left(\frac{r_{\alpha\alpha'}}{r} \right)^6 \right], \quad (1)$$

with the parameters that depend on the type of interacting atoms and the usual truncature to $r \leq r^* = 1.49 r_{\alpha\alpha'}$ to avoid the problem of long range interactions in the simulations. Between two substrate atoms we use $V_{ss} = 3$ and the equilibrium distance is $r_{ss} = 3$. The interaction between the substrate and the lubricant is always much weaker with $V_{sl} = 1/3$. For the lubricant itself, we consider two cases henceforth denoted by “soft lubricant” and “hard lubricant” although, in both cases, the lubricant is less rigid than the two substrates. The soft lubricant uses $V_{ll} = 1/9$ and describes the case of a lubricant made of very weakly interacting molecules. The hard lubricant uses $V_{ll} = 1$. The equilibrium distance between lubricant atoms is $r_{ll} = 4.14$, i.e., it is “incommensurate” with the equilibrium atomic distance in the substrate. The parameter r_{sl} characterizing the interaction be-

tween the substrate and the lubricant is $r_{sl} = \frac{1}{2}(r_{ss} + r_{ll})$. The atomic masses are $m_l = m_s = 1$. All the parameters are given in dimensionless units defined in Ref. [13]. The two substrates are pressed together by a loading force, which is equal to $f_{\text{load}} = -0.1$ per atom of the top substrate layer, except where otherwise specified.

While the model characteristics presented above are fairly standard for molecular dynamics simulations, the main difference between our calculations and other simulations of confined materials [9,10,14] lies in the coupling with the heat bath, i.e., part of the material, which is not explicitly included in the simulation. We use Langevin dynamics with a damping coefficient η , which has been designed to mimic a realistic situation, and is presented in details in Ref. [13]. In a system such as the one that we simulate, the energy loss comes from the degrees of freedom that are not included in the calculation, i.e., the transfer of energy to the bulk of the two substrate materials. Therefore, the damping must depend on the distance z between an atom and the substrate. Moreover, the efficiency of the transfer depends on the velocity v of the atom because it affects the frequencies of the motions that it excites within the substrates. The damping is written as $\eta(z, v) = \eta_1(z) \eta_2(v)$ with $\eta_1(z) = 1 - \tanh[(z - z^*)/z^*]$, where z^* is a characteristic distance of the order of the lattice spacing. The expression of $\eta_2(v)$ is deduced from the results known for the damping of an atom adsorbed on a crystal surface. It includes a frequency-dependent phonon term and an additional damping due to the creation of electron-hole pairs in the substrate [13].

The procedure chosen for our molecular dynamics experiments is inspired from the procedure that one would carry in an actual experiment. Samples are “prepared” at low temperature and then they are slowly heated in a series of simulations while their properties are monitored.

The first step is, therefore, the preparation of a suitable initial configuration for the simulation. This requires some care because, as the substrate and the lubricant have incommensurate equilibrium distances, the equilibrium structure is not known *a priori*. The structure of the substrates is determined by the top and bottom layers that are kept rigid. For these two layers we chose a square lattice with a lattice spacing corresponding to the equilibrium distance r_{ss} . The initial configuration of the two deformable layers of the substrate have the same square lattice structure. The initial configuration of the lubricant is a set of N_l layers with an initial triangular structure and a lattice spacing equal to r_{ll} , and a size in the x, y directions selected to the optimal match with the periodic boundary conditions that we use. Most of the simulation have been performed with an initial condition having 80 atoms in each lubricant layer. Calculations with systems having their sizes doubled in one or both horizontal directions have confirmed that the results are not sensitive to the system size.

Then this initial configuration is used for a simulation at $T=0$. As the system is dissipative, it tends to relax to a steady-state minimum energy configuration. However, this configuration is not necessarily the ground state of the system because such incommensurate lattices have many metastable configurations. Sequences of heating and slow cooling

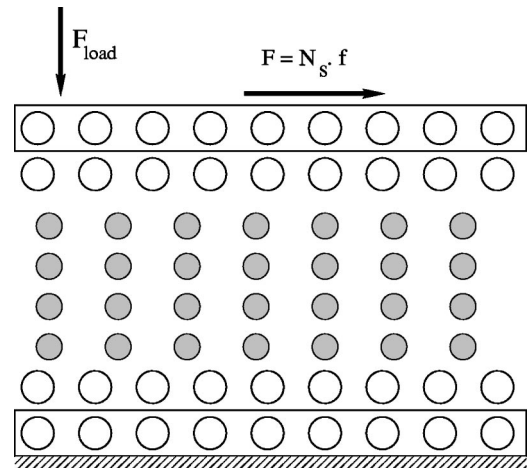


FIG. 1. Schematic picture of the model. The gray circles show the lubricant atoms, while open circles show the substrate atoms. The enclosed atoms in the two substrates correspond to the rigid parts of the substrate while the dynamics of the other substrate atoms is fully simulated. The load and, in some cases, shear forces are applied to the rigid part of the top substrate, as shown by the arrows. The rigid part of the bottom substrate is fixed.

have been used to anneal the system. An efficient relaxation to the ground state is achieved if these sequences are carried in the presence of a small dc shear force applied to the top substrate, as shown in Fig. 1.

A crucial issue for such a calculation is the choice of the boundary conditions. One can either work with a fixed number of particles, i.e., a fixed film density, as we do here, or a fixed chemical potential. Grand canonical simulation methods have been designed: earlier work [15] used the Monte Carlo methods to maintain a fixed chemical potential, but dynamical studies are also possible by the introduction of a particle reservoir [16,17]. The choice between canonical and grand canonical simulations is important because density changes influence phase changes. The optimal choice depends on the time scales of the phenomena of interest with respect to the typical time necessary for molecular transport. We are interested in confined melting in the context of friction because a sequence of melting-freezing transitions has been proposed as a source of the microscopic stick slip, which is observed in numerical simulations and therefore occurs on a microscopic time scale [1,2]. In a typical macroscopic experiment with a steel block of 10^3 cm^3 , the actual contact area can be as low as 0.1 mm^2 and include $10^3 - 10^5$ contacts [1]. Therefore, the linear size of a single contact is $r \leq 0.01 \text{ mm}$, which is very large at the molecular scale ($r \sim 10^4$ in our units). As discussed below (see, for instance, Fig. 6) a typical value for the diffusion coefficient in our calculations is $D \approx 10^{-4}$, which implies that the typical time for diffusion over a contact is 10^{12} in our units, i.e., much larger than the time of interest (and observable) in our calculations. Such a very long diffusion time corresponds to the fact that actual contacts are very large at the atomic scale. The region that we simulate should be viewed as only a small piece of a much larger contact area. The particle reservoirs, which are indeed present in an actual physical situ-

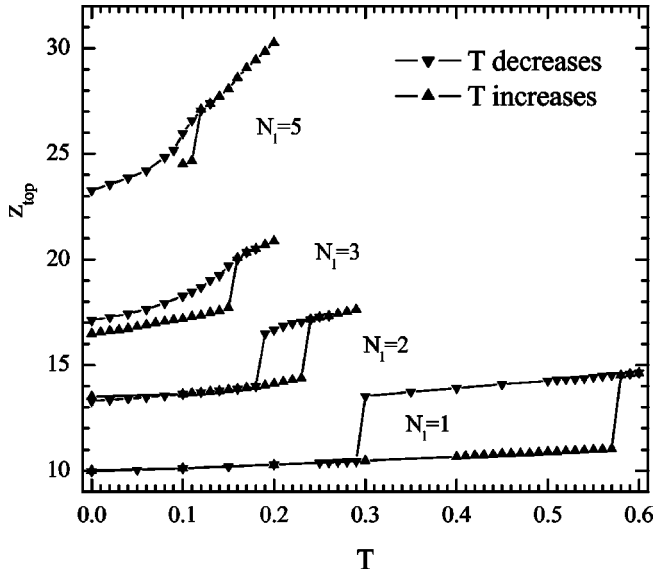


FIG. 2. Vertical coordinate Z_{top} of the top substrate as a function of temperature for different lubricant film thicknesses, in the case of a “soft lubricant.”

ation, are too far to have an essential effect on the time scale of a simulation (or the time scale of microscopic stick slip). These orders of magnitude are of course only very rough, in particular, because a real contact is not flat at the atomic scale on a very large area, but the gap between the diffusion time scale and the time scale relevant for our applications is so large that the conclusion still holds and the constant particle number condition appears to be the most appropriate for our problem. This would not be the case in simulations addressing truly equilibrium properties such as the understanding of solvation forces as in Refs. [16,17]. On the other hand, contrary to the previous grand canonical simulations [15–17] that were performed with a fixed distance between the confining walls, the z coordinate of the top substrate is a variable here. This has important consequences on the structure of the film, and corresponds to the actual situation in friction.

III. SOFT LUBRICANT BETWEEN PERFECTLY FLAT CONFINING SURFACES

Let us first consider the case of a soft lubricant ($V_{ll} = 1/9$) that corresponds to the typical situation of a molecular film between two solid substrates.

Molecular dynamics (MD) simulations can provide detailed information on the displacements of all atoms but, in order to compare the results with the experiments, it is also useful to extract some global variables that describe the system at a mesoscopic scale. An important characteristic parameter of the lubricant, connected to its thermodynamic state, is its specific volume. For the confined lubricant that we study here, only the thickness of the lubricant film can change and, therefore, the variation of the specific volume shows up in the variation of the vertical coordinate Z_{top} of the top substrate. Figure 2 shows the variation of Z_{top} when the initial configuration prepared as described above is slowly heated and then slowly cooled down.

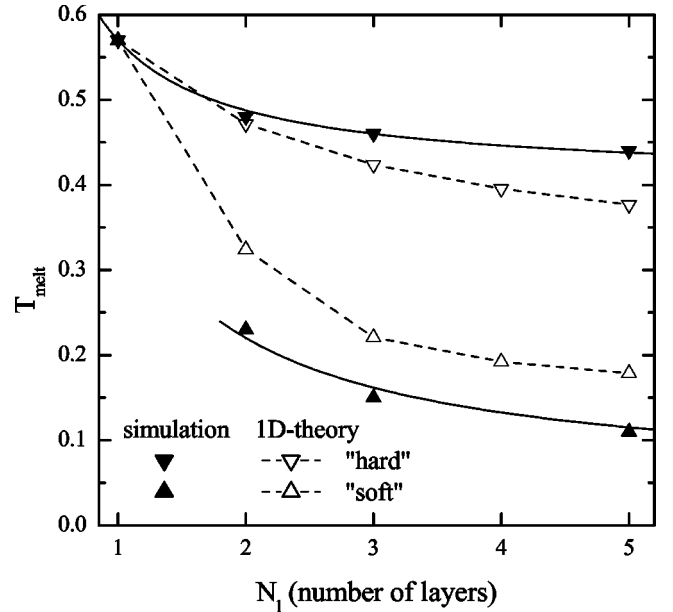


FIG. 3. Evolution of the transition temperature T_m as a function of the number of lubricant layers for $f_{\text{load}} = -0.1$. The filled markers correspond to MD simulation results, while the open markers are the theoretical values discussed in Sec. VI. The solid curves describe the fits $T_{\text{melt}} = 0.405 + 0.165/N_l$ for the hard lubricant and $T_{\text{melt}} = 0.045 + 0.350/N_l$ for the soft lubricant.

For all the lubricant thicknesses that have been investigated ($N_l = 1$, to, 5 layers), the general behavior of the system is the same. On heating a sharp increase of Z_{top} is observed at a temperature T_m that depends on N_l , as shown in Fig. 3. On cooling the behavior depends on the number of lubricant layers: for $N_l = 1$ or 2, a sharp transition that brings the system back to the values observed upon heating is found, while for larger values of N_l , Z_{top} decreases slowly toward the values found upon heating.

It is interesting to compare our results with the known properties of a bulk lattice of particles interacting with Lennard-Jones potentials, that have been obtained by the Monte Carlo calculations [18]. With the appropriate rescaling of the parameters and for the pressure that results from the loading force $f_{\text{load}} = -0.1$ per unit cell of the substrate that we have used, the melting transition of the bulk lattice is found at $T = 0.044$ and it is associated to a relative change in the specific volume $(v_{\text{liquid}} - v_{\text{solid}})/v_{\text{solid}} = 0.112$. For a soft lubricant, the transition temperature T_m versus N_l , shown in Fig. 3, is well fitted for $N_l \geq 2$ by the expression $T_m = 0.045 + 0.350/N_l$, which is in very good agreement with the bulk results when N_l becomes large. The relative volume change, equal in our case to $\Delta Z_{\text{top}}/Z_{\text{top}}$ where Z_{top} is the value at the bottom of the jump and ΔZ_{top} is the variation of Z_{top} at the jump, varies from 0.136 for a three-layer lubricant to 0.098 for a five-layer lubricant. Therefore, the transition that we observe upon heating appears to be consistent with the melting transition, perturbed by the substrate, but its exact nature needs, however, to be precised.

In order to better understand the phenomena that occur at this transition, it is useful to look at the trajectories of the particles in the vicinity of the transition point. When the

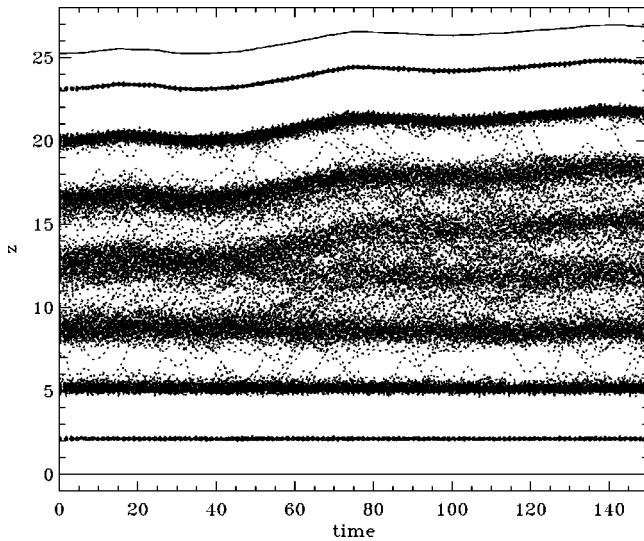


FIG. 4. Time evolution of the positions along z of all the particles for a soft lubricant with $N_l=5$ at temperature $T=0.12$.

temperature is raised to T_m from a slightly lower value, a transient during which Z_{top} keeps a value close to its previous value is observed, but then, in a short time domain, Z_{top} raises to its stable value at T_m , as shown in Fig. 2. The trajectories of the particles show that the increase of film thickness is due to the *formation of an additional layer in the film*. It is interesting that a sharp transition between the two film thicknesses that differ by one molecular layer has also been observed experimentally [3] in careful investigations of highly confined thin organic films, studied with a surface force balance. In these experiments, carried at constant temperature, this sharp transition was due to a change in the confinement.

Before calling “melting” the transition that corresponds to a strong increase of the specific volume of the lubricant, additional checks are necessary because, in such a highly confined environment, the frontier between the liquid and solid states is not as well defined as in the bulk. Looking at Fig. 4 one can notice that even in the high temperature “liquid” phase the lubricant is still organized into layers. Such a behavior has been experimentally observed for fluids in the immediate vicinity of a solid [7] and, therefore, is not inconsistent with a liquid phase at $T > T_m$. To confirm the nature of the transition, it is useful to investigate another characteristic of the lubricant layer, its shear modulus.

For this purpose, numerical simulations with a small amplitude constant shear force were performed. Figure 5 shows that below T_m the lubricant behaves like a rigid body, with only a negligible displacement under the shear stress, while, for $T > T_m$, the top substrate takes a nonzero equilibrium velocity, indicating a fluid lubricant.

Müser and Robbins have pointed out recently [19] that for the commensurate substrates such as used in our simulation, the static frictional force should be nonzero even in the case of a fluid lubricant film. Indeed, the periodic potential of one surface induces a commensurate density modulation parallel to the surface in the lubricant. The magnitude of the density modulation decreases exponentially with the distance from

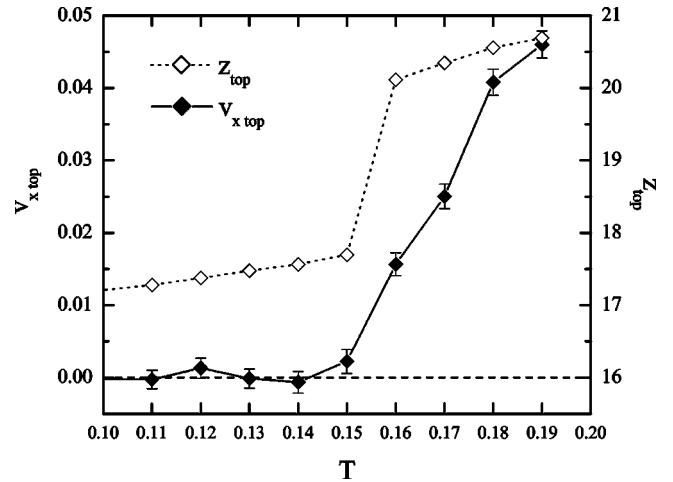


FIG. 5. Comparison between the temperature variation of Z_{top} and of the equilibrium velocity of the top substrate when a small shear stress, $f=0.001$ per substrate atom, is applied to the system (soft lubricant, $N_l=3$).

the first surface, but remains finite, and the second surface whose periodicity is commensurate with this modulation, should always feel a periodic force that pins the substrates together. The magnitude of this pinning, however, is too small to be detected in our simulation. As we see from Fig. 5, the mobility demonstrates a rather sharp increase exactly at the melting temperature.

These results seem to clarify the picture because they show that T_m is a temperature that separates a rigid phase from a fluid phase that has a specific volume, which is significantly higher but nevertheless of the same order of magnitude. Therefore, T_m appears as a solid-liquid transition temperature, and can therefore be called the “melting temperature” of the confined lubricant. However, the properties of the “solid” lubricant phase are not trivial. This is shown in Fig. 6(a). Following trajectories of the particles in the MD simulation, one can notice many jumps from one lubricant layer to another, even at temperatures $T \ll T_m$. The high mobility of the lubricant atoms is also attested by the calculation of their diffusion coefficient versus T . The diffusion coefficient in one direction (for instance x) is evaluated by calculating $\langle x^2 \rangle - \langle x \rangle^2$ versus time, where $\langle \cdot \rangle$ indicates an averaging over all lubricant atoms, and then fitting its value by a linear dependence of slope D_x . We have calculated the average diffusion coefficient parallel to the layers D_{\parallel} and the diffusion coefficient orthogonal to the layers D_z , which is one order of magnitude smaller than D_{\parallel} but nonzero, and shows a similar temperature variation. As one might expect the diffusion coefficient increases sharply when T reaches the melting temperature, it is, however, already rather large for $T < T_m$. In this domain its temperature dependence is approximately fitted by an Arrhenius law $D \propto \exp(-E_a/T)$ with $E_a \approx 0.16$, indicating an activated process. It is interesting to notice that the activation energy is approximately equal to the melting temperature (expressed in energy units). This result is again consistent with experiments: recent experimental observations using fluorescence correlation spectroscopy in molecularly thin confined films that display static friction

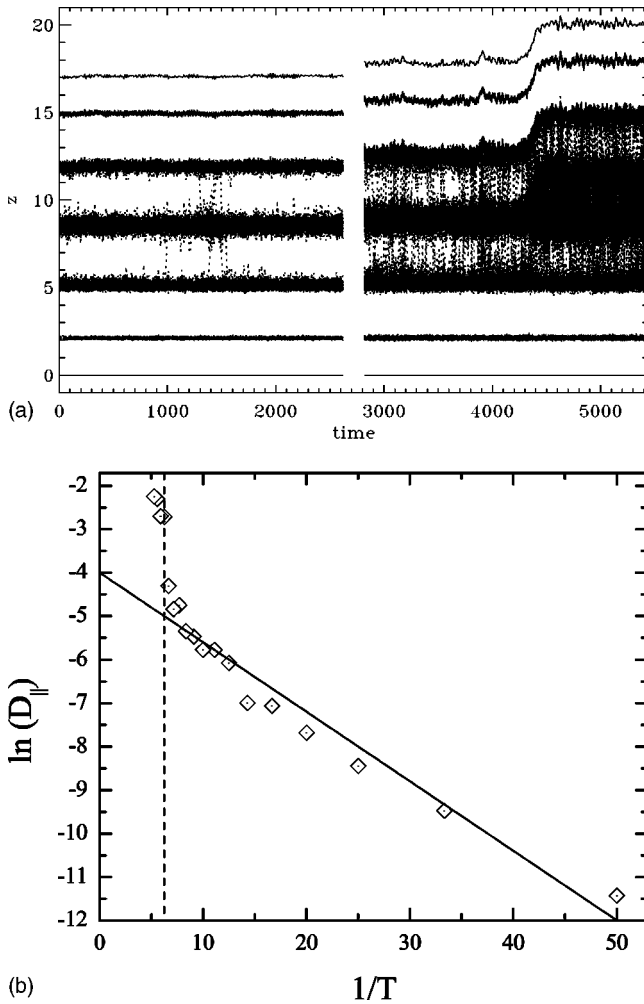


FIG. 6. (a) Time evolution of the z coordinates of the particles at temperatures $T=0.08$ (left part of the figure) and 0.16 (right part of the figure) for a soft lubricant. The vertical lines that connect the layers show that particles are changing layers. At $T=0.16$, the time snapshot has been centered on the moment where the system melts by creating a new layer. The figure shows that the transitions of the particles between layers increase with melting, but there is nevertheless not a large qualitative change when the melting occurs. (b) Diffusion coefficient of the particles along the layers D_{\parallel} vs inverse temperature in semilogarithmic scales.

[4] have found that diffusion is large. The role of confinement to induce “solidification” in a fluid is often mentioned [1–3] and, in our calculations this is confirmed by the increase of the melting temperature when N_l decreases. However, MD simulations as well as the experiments also point out an effect that appears to be less appreciated: the mobility of the atoms in a highly confined solid is much greater than that in a bulk solid phase. This can be understood qualitatively by the influence of the substrate that distorts the perfect solid configuration because it is generally incommensurate with the solidified film. As shown in Fig. 7, the solid phase of the film is not a perfect crystalline state. It is formed of rather well-ordered domains separated by regions that appear like grain boundaries, or discommensurations. Within these discommensurations the atomic density is generally

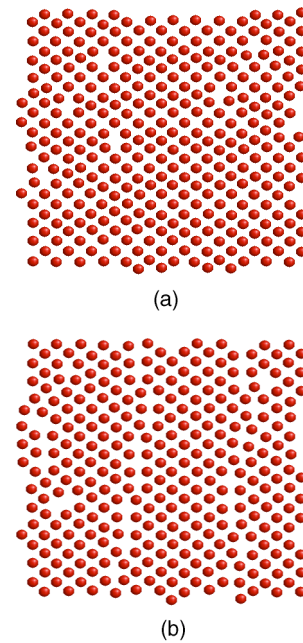


FIG. 7. Equilibrium structure at $T=0$ of the top (a) and middle (b) layers in a three-layer soft lubricant film ($N_l=3$). (Figures produced with RasTop [22].)

lower than in the ordered domains, leaving vacant space for diffusion. The existence of mobile particles within a “solid” confined phase has also been observed in MD simulations of ultrathin films confined between corrugated walls [20]. In such a system the film consists of fluid-filled nanocapillaries separated by solids strips. As shown by a recent experimental study [21], surface corrugation, due to the presence of nanoparticles, could also play some role in the experimental observations of Ref. [4].

Our results show that a similar phenomenon can exist even in the absence of corrugation due to the incommensurability between the film and the walls. The basic physics between the process is the same: the conditions of the confinement induce some frustration in the film that lead to this hybrid “solid-fluid” structure.

When one cools down the melted film, Fig. 2 shows that it does not retrace the path observed upon heating. For very thin films ($N_l=1$ or 2), a sharp freezing transition is observed at a temperature significantly lower than T_m . After the transition the film recovers the structure that it had at the same temperature before the melting transition. Therefore, in these cases one simply notices a large hysteresis between melting and freezing, as could be expected for the first-order melting transition. Thicker films show a more complex behavior because they freeze in a metastable state. Figures 8(a) and 8(b) show sample configurations for a film having initially three layers ($N_l=3$). In Fig. 8(a), one notices that a defected four-layer configuration persists below T_m , and when the film is cooled down to $T=0$, a configuration having three layers in one region and four layers in another is found. Such a configuration is of course not an equilibrium configuration, and annealing in the presence of a small shear brings the film back to its equilibrium state. The qualitative

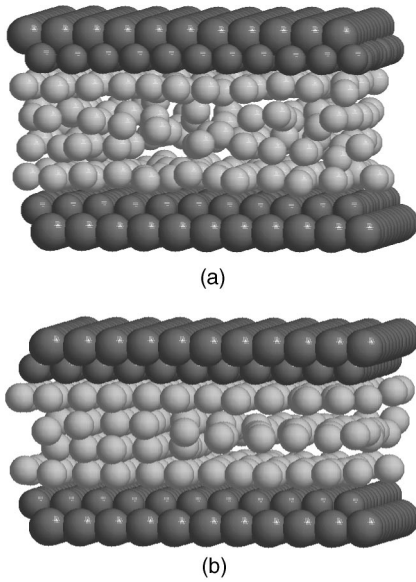


FIG. 8. Configurations of a soft lubricant with $N_l=3$ upon freezing: (a) $T=0.13$ and (b) $T=0$. (Figures produced with RasTop [22].)

difference between the behaviors observed for narrow films ($N_l=1$ and 2) and thicker ones ($N_l \geq 3$) is due to the influence of the substrate. For $N_l=1$ or 2, all the layers interact with the substrates which tend to impose a given configuration, which is not the case for thicker films. The specificity of $N_l=2$ with respect to higher values was also noticed in the experiments attempting to decrease the thickness of a lubricant film by applying a strong pressure [3]. Pressure alone is not sufficient to decrease it below $N_l=3$, but, by applying additionally a shear stress, the lubricant width can be decreased down to two layers. This is exactly what we find for the relaxation of the film on cooling.

IV. HARD LUBRICANT

The case of “hard lubricant” ($V_{ll}=1$) shows some similarities with the results discussed in Sec. III but also significant differences, as shown in Fig. 9. First, one should notice that the denomination hard is used in comparison with the previous case, but the binding energy of two lubricant atoms is still lower than that of the substrate atoms (by a factor of 1/3). As for the soft lubricant, we find a melting transition at a temperature T_m that decreases when the thickness of the film increases (Fig. 3). As expected because the interaction is stronger, melting occurs at higher temperatures than for a soft lubricant. The melting mechanism is similar for hard and soft lubricants: it occurs by the formation of one additional layer (Fig. 10), but for a hard lubricant the hysteresis on cooling is much larger and the barrier between the metastable state with N_l+1 layer and the equilibrium state of the film is much higher, so that on freezing the film always stays in a metastable state with N_l+1 layer. These results suggest that, while the basic physics is similar for hard and soft lubricants, there are, however, some qualitative differences that can be related to the greater depth of the secondary minima

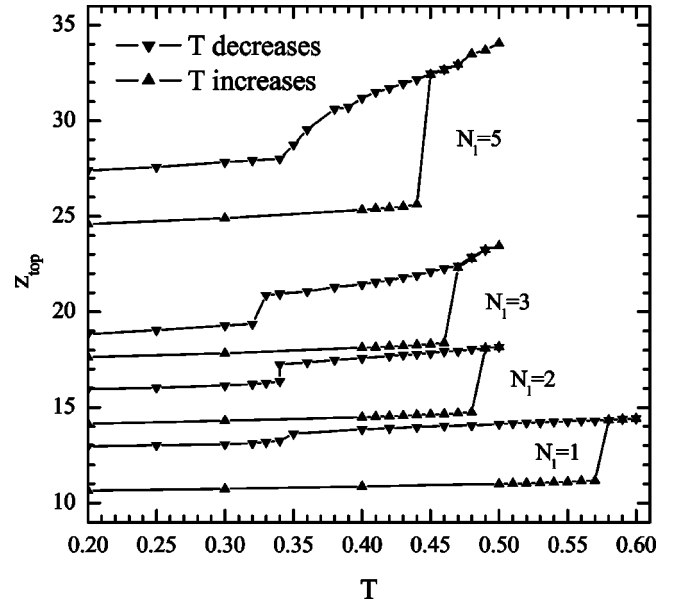


FIG. 9. Vertical coordinate Z_{top} of the top substrate as a function of temperature for different lubricant film thicknesses, in the case of a “hard lubricant.”

of the potential energy surface that correspond to metastable states and to the fact that the hard lubricant is less perturbed by the substrate. For instance, we did not observe atomic jumps between layers below T_m for the hard lubricant. The low temperature phase is, therefore, closer to what one expects for a bulk solid. This is also consistent with smaller variations of T_m versus N_l for a hard lubricant than that for a soft one.

V. INFLUENCE OF THE QUALITY OF THE CONFINING SURFACES

In an actual experiment, it is very hard to achieve perfectly smooth confining surfaces and some imperfections can be present even on surfaces prepared with great care [21]. It is, therefore, important to study the effect of the modulation of the film thickness. We have performed some simulations with a curved top substrate for which the z coordinates varies along the x direction by $\Delta z = \frac{1}{2} h_x r_{sl} (1 - \cos 2\pi x/L)$, where L is the size of the substrate and $h_x=1$ in the results shown here. An example of a configuration with a curved substrate is shown in Fig. 11. Figure 12 shows that the curvature of the substrate has a profound effect on the melting transition. In most of the cases the associated to a jump in Z_{top} is no longer observed in the MD simulations and is replaced by a smooth evolution. The observation of the configuration of the particles in Fig. 11 suggests an explanation for this observation. The spatial variation of the thickness of the film leads to the coexistence of domains that do not have the same number of layers. From the results with flat substrates we know that the melting of these domains should occur at different temperatures, thicker regions melting first. In the curved system the thicker regions presumably start to melt first and then drive the melting of the thinner regions. And moreover, as the boundary between domains with different thicknesses is full

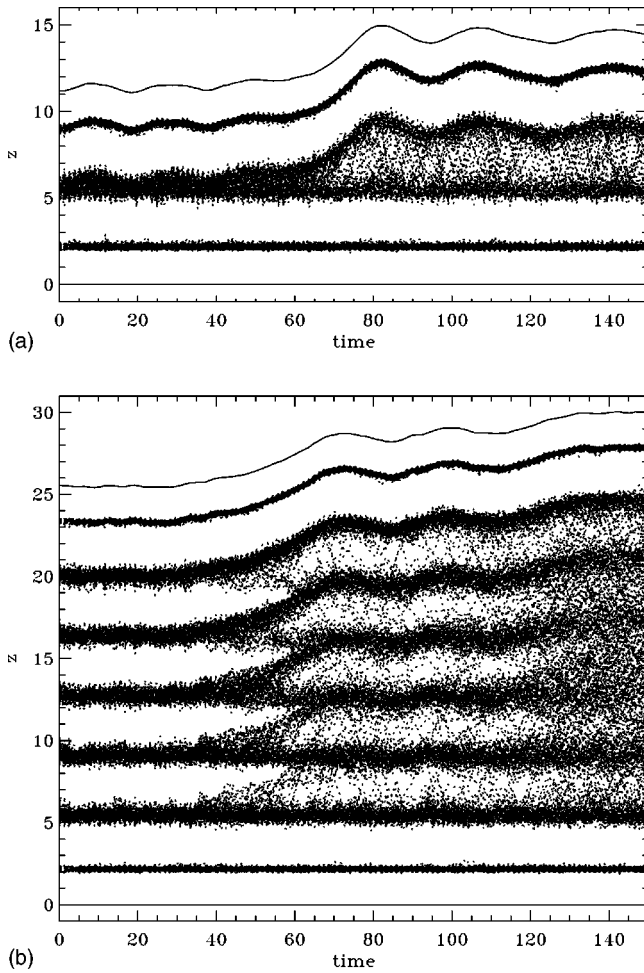


FIG. 10. Time evolution of the positions along z of all the particles for a hard lubricant with $N_l=1$ at temperature $T=0.58$ (a) and $N_l=5$ at temperature $T=0.45$ (b).

of defects in the atomic packing, they also contribute to preventing a well-defined transition, and the melting is blurred.

However, the effect of substrate curvature is certainly greatly exaggerated by the small size of the system that can be simulated in MD. In an actual experiment one can expect that flat surfaces will extend over hundreds, or even thousands, of lattice spacing, allowing melting to occur rather sharply in each of the regions. Therefore, one can expect that a melting transition should actually be observed even with imperfect substrates, but it will not be very sharp.

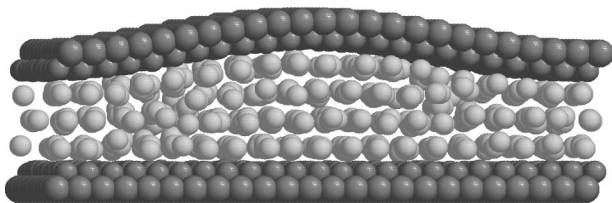


FIG. 11. Example of a configuration with a curved top substrate for a hard lubricant, $N_l=3$ at $T=0.37$. (Figure produced with Ras-Top [22].)

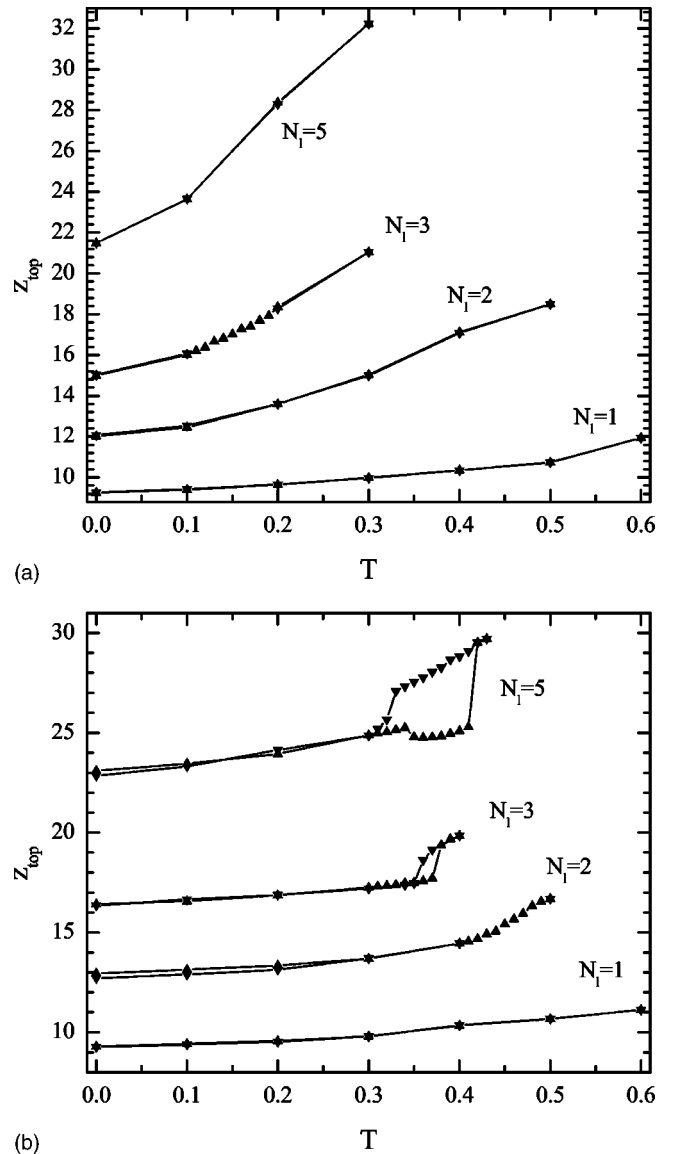


FIG. 12. Vertical coordinate Z_{top} of the top substrate as a function of temperature for different lubricant film thicknesses, for curved substrates ($h_x=1$): (a) soft lubricant, (b) hard lubricant. The triangles pointing up correspond to the points recorded upon heating, while those pointing down were obtained upon cooling.

VI. PHENOMENOLOGICAL THEORY

The MD simulation results have shown that melting is strongly affected by the confinement. The solid and fluid phases are different from their bulk counterpart because the solid shows large atomic mobility while the liquid is partly ordered into layers, but the most noticeable effect of the confinement is to change the melting temperature by a large amount that depends on the film thickness, as shown in Fig. 3. The theoretical explanation of this result is difficult because there is no exact theory of the solid-liquid transition even in the bulk case. A mean-field theory for the confinement-induced first-order phase transitions was recently proposed [12]. It is based on a Ginzburg-Landau expression for the free energy that contains a phenomenologi-

cal surface correction, which has the same double-well shape as the bulk free energy contribution that leads to a first-order transition, but has different coefficients that amounts to saying that the surface layer has preference to order at a higher temperature than in the bulk. Such a theory is interesting because it provides a thermodynamic picture of the effect of the confinement, but it is hard to relate to our results because its parameters cannot be determined for a given material. Another approach relies on the empirical Lindemann criterion, which states that melting starts when the amplitude of mutual displacement of nearest neighboring atoms reaches some threshold value, $u_{l,l'}^2 \equiv \langle (u_l - u_{l'})^2 \rangle = \beta_L^2 a^2$. The coefficient β_L depends on the material; however, it is remarkable that it only varies in a small range and stays around $\beta_L \sim 0.1$ [23], justifying the validity of the Lindemann criterion as an empirical characteristic of the melting point. At higher amplitude of vibrations the anharmonicity effects become too strong and destroy the crystalline order. In the case of a thin film, mutual displacements are expected to increase for a film with a free surface (or the free-slip boundary condition for the lubricant-substrate interface), or to decrease for the “stick” boundary condition, when the oscillations of the boundary atoms of the confined film are suppressed. Therefore, one expects a decrease of the melting temperature (comparing with the bulk value) in the former case and the increase of T_{melt} in the later one. Such a theory was developed by Tkachenko and Rabin [11]. It predicts that for the “stick” boundary condition the melting temperature increases as

$$\Delta T_{\text{melt}}(N_l)/T_{\text{melt}}^{(\text{bulk})} \approx C/N_l \quad (2)$$

with a coefficient $C \approx 1$. If we fit our simulation results with such an expression, the fit is qualitatively correct, but the coefficient C is very different from 1 (0.41 for the hard lubricant and 7.8 for the soft lubricant).

The possible problem of the theory of Tkachenko and Rabin is that it evaluates the thermal fluctuations with a continuous-medium elasticity theory. While this approach is qualitatively correct, for a lubricant film containing only a few layers, it is only approximate.

Let us show that a microscopic theory of the phonon spectrum of the confined film leads to a much better agreement with the simulation.

A general approach to the calculation of the phonon spectrum is to use the Green-function technique (e.g., see Ref. [24,25]). The causal phonon Green function is defined by

$$G(t; l, l') = \frac{\sqrt{m_l m_{l'}}}{i\hbar} \langle T_{\text{ch}} u_l(t) u_{l'}(0) \rangle, \quad (3)$$

where $u_l(t)$ is the displacement of the l th atom from the equilibrium position in the Heisenberg representation, m_l is its mass, and T_{ch} is the chronological operator. The Fourier transform of $G(t)$ satisfies the equation

$$(\Omega^2 \mathbf{1} - \mathbf{D}) \mathbf{G}(\omega) = \mathbf{1}, \quad (4)$$

where $\Omega^2 = \omega^2 + i\epsilon$, $\epsilon > 0$, $\epsilon \rightarrow 0$. The dynamical matrix \mathbf{D} is a square matrix with the elements $d_{l,l'} = \alpha(l, l') / \sqrt{m_l m_{l'}}$. For a pairwise interatomic potential V , $\alpha(l, l')$ are defined as

$$\alpha(l, l') = \frac{\partial^2 V(x_l - x_{l'})}{\partial u_l \partial u_{l'}} \quad \text{if } l \neq l' \quad (5)$$

and

$$\alpha(l, l) = \sum_{l'' (l'' \neq l)} \frac{\partial^2 V(x_l - x_{l''})}{\partial u_l^2}. \quad (6)$$

The power of the Green-function technique is that additional contributions to the dynamical matrix can be accounted consequently, one by one, with the help of the Dyson equation. Namely, if \mathbf{G}_0 is a solution of $(\Omega^2 \mathbf{1} - \mathbf{D}_0) \mathbf{G}_0 = \mathbf{1}$, the solution of Eq. (4) is given by

$$\mathbf{G} = \mathbf{G}_0 + \mathbf{G}_0 \delta \mathbf{D} \mathbf{G}, \quad (7)$$

where $\delta \mathbf{D} = \mathbf{D} - \mathbf{D}_0$ is the correction to the dynamical matrix. Therefore, one may start with a simple case, for instance, of an infinite lubricant crystal, and then introduce the substrates as described below.

When the Green function is known, the correlation function can be calculated as

$$\langle u_l u_{l'} \rangle = - \frac{2k_B T}{\pi \sqrt{m_l m_{l'}}} \int_0^\infty \frac{d\omega}{\omega} \text{Im} G(\omega; l, l'), \quad (8)$$

and then the mutual displacements are given by $u_{l,l-1}^2 = \langle u_l^2 \rangle + \langle u_{l-1}^2 \rangle - 2\langle u_l u_{l-1} \rangle$.

Now let us apply this technique to the simplest one-dimensional model of the confined film; namely, we represent each lubricant layer as a single “particle” of mass m at the node l ($l = 1, \dots, N$), and the rigid substrates, as two “particles” of infinite mass situated at the nodes $l = 0$ and $l = N + 1$. Let the interaction between the nearest neighboring “layers” be described by the harmonic potential $\tilde{V}_{ll}(z) = \frac{1}{2} g_{ll} z^2$, and that between the lubricant and the substrate, by the potential $\tilde{V}_{sl}(z) = \frac{1}{2} g_{sl} z^2$. For the Lennard-Jones potential used in the simulation, we have for the elastic constants $g_{\alpha\alpha'} = 72V_{\alpha\alpha'} / r_{\alpha\alpha'}^2$ ($\alpha = s, l$) in the case of a zero load.

Let us start from the infinite one-dimensional chain of lubricant “layers.” In this case the nonzero elements of the dynamical matrix are $\alpha(l, l) = 2g_{ll}$ and $\alpha(l, l \pm 1) = -g_{ll}$, and the Green function is given by the expression

$$G_0(\omega; l, l') = - \frac{2i}{\omega_m^2} \frac{(-\xi + i\sqrt{1-\xi^2})^{|l-l'|}}{\sqrt{1-\xi^2}}, \quad (9)$$

where $\omega_m = 2\sqrt{g_{ll}}$ is the maximum phonon frequency of the chain and $\xi = 2\Omega^2/\omega_m^2 - 1$. Now, let the mass of the “particle” with the index $l = 0$ be changed to $m_0 = m + \Delta m$. The nonzero perturbations in this case are $\delta D(0, 0) = \alpha(0, 0)(m_0^{-1} - m^{-1})$ and $\delta D(0, \pm 1) = \alpha(0, 1)[(m_0 m)^{-1/2} - m^{-1}]$. For the rigid substrate we substitute $m_0 = \infty$, so that

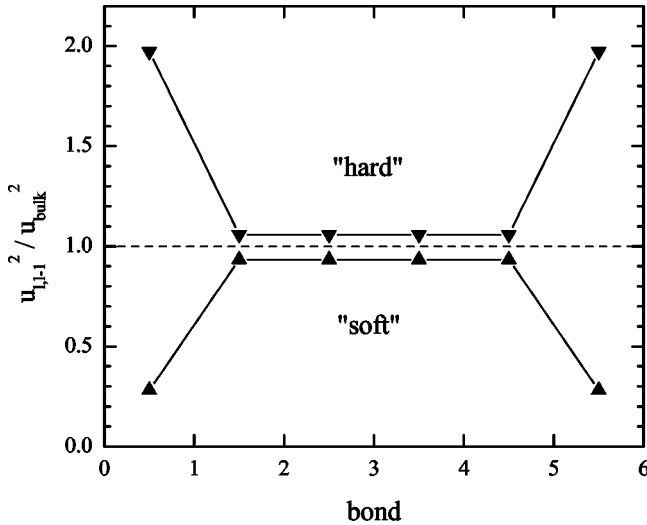


FIG. 13. Mutual displacements of the “layers” in the one-dimensional (1D) model for the $N_f=5$ lubricant film.

the perturbations reduce to $\delta D(0,0) = -2g_{ll}$ and $\delta D(0, \pm 1) = g_{ll}$. Then the Dyson equation (7) can be solved in the following three steps: first, the subsystem of two equations for $G(0,0)$ and $G(1,0) = G(-1,0)$ decouples from the whole set of equations and can be easily solved; second, we can find the functions $G(l,0)$ and $G(l, \pm 1)$; and finally, the function $G(l, l')$ for arbitrary l, l' can be obtained from Eq. (7). The second “substrate” at the node $l=N+1$ is introduced in the same way.

In the next step, we change the bonds between the lubricant and the substrates, namely, if the interaction between the $l=0$ and $l=1$ particles is changed, $\delta \tilde{V}(z_1 - z_0) = \frac{1}{2}(g_{sl} - g_{ll})(z_1 - z_0)^2$, then the perturbations are $\delta D(0,0) = \delta \alpha(0,0)/m_0$, $\delta D(1,1) = \delta \alpha(1,1)/m$, and $\delta D(0,1) = \delta \alpha(0,1)/\sqrt{m_0 m}$, and in the case of the rigid substrate, $m_0 = \infty$, the only nonzero perturbation of the dynamical matrix is $\delta D(1,1) = g_{sl} - g_{ll}$. Similarly, the change of the interaction with the top substrate leads to the perturbation $\delta D(N,N) = \delta D(1,1)$, and the Dyson equation (7) may be solved in the same way as above.

The mutual displacements of the layers across the lubricant calculated in this way for the parameters used in the simulation ($V_{sl} = 1/3$, $V_{ll} = 1$ for the hard lubricant and $V_{ll} = 1/9$ for the soft one) are presented in Fig. 13. As expected, the mutual displacement is maximal at the interface for the hard-lubricant case, and at the middle of the film in the soft-lubricant case, which has internal interactions weaker than its interactions with the substrates.

Now, using the Lindemann criterion, we may assume that in the hard-lubricant system the melting starts when $u_{1,0} = \beta_L r_{sl}$ (the melting starts at the interface), while in the soft-lubricant case the melting temperature is determined by the condition $u_{l+1,l} = \beta_L r_{ll}$ for $l=N/2$ (the melting starts in the middle of the lubricant). Taking $\beta_L = 0.0966$ for the Lindemann constant, which is chosen so that the theoretical and numerical values of the melting temperatures agree for the one-layer film $N_f=1$, we obtain the results presented in Fig. 3. One can see that the agreement between the simulation

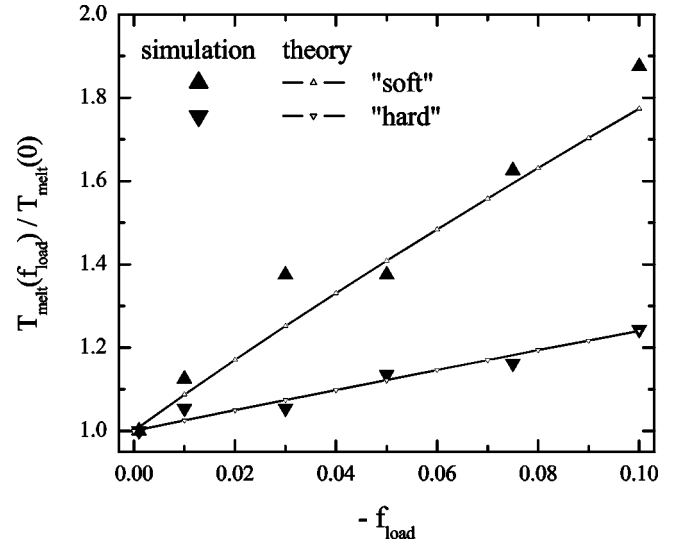


FIG. 14. Dependence of the melting temperature on the load for the $N_f=3$ system: comparison of the 1D theory with simulation results.

and theory is fairly good although we did not use any fitting parameter, except for the value of the Lindemann constant, which has been obtained from a single point on the curves and takes a value that corresponds very well to the expected value $\beta_L \sim 0.1$, which is observed for most of the solids.

The approach described above can also be used to study the effect of the external pressure. When $f_{load} \neq 0$, the particles lie at the minimum of the potential $V_f(z) = V_{LJ}(z) - z f_{load}$, which corresponds to a new equilibrium distance r_f obtained from the nonlinear equation $(\gamma^6 - 1)\gamma^7 + (f_{load} r_{\alpha\alpha'}) / (12V_{\alpha\alpha'}) = 0$ for the variable $\gamma \equiv r_{\alpha\alpha'} / r_f$. Then one can calculate the new elastic constant as $g_f = V''_{LJ}(r_f)$. When the load grows, the equilibrium distances decrease and, due to the anharmonicity of the Lennard-Jones potential, the elastic constants increase. This leads to the increase of the melting temperature with load, as shown in Fig. 14.

Taking into account that the interaction between the lubricant layers is the sum of individual interactions between the atoms in these layers and not a simple Lennard-Jones interaction of two atoms (or at least the parameters of this effective interaction have to be changed), the agreement between the results predicted by the simplest 1D model and the simulation ones is surprisingly good. One reason for this is that our system is close to the harmonic regime: as we checked, for all temperatures the kinetic and potential energies of the system are very close to each other. Thus, from the consideration presented above, we can conclude that (1) the melting of the confined film is mainly governed by normal vibrations of the atoms, and (2) the melting starts from the interface layers in the case of the hard lubricant and from the middle layer in the case of the soft lubricant.

The approach described above can be generalized to a three-dimensional system in a straightforward way, although the calculations become too heavy to be performed without the help of a symbolic manipulation program. First, one has to find the spectrum $\Omega_0(\kappa)$ of an isolated two-dimensional

lubricant layer, which now depends on the two-component wave vector $\kappa \equiv (k_x, k_y)$ [e.g., for the square lattice one has $\Omega_0(\kappa) = 2\omega_m \sin(ak_x/2)$ for the x component of the displacements], and make the substitution $\Omega^2 \rightarrow \Omega^2 - \Omega_0^2(\kappa)$ in Eq. (9). Second, one should make additionally the two-variable integration $(a/2\pi)^2 \int \int_{-\pi/a}^{\pi/a} dk_x dk_y \dots$ in Eq. (8). Finally, we have to distinguish the x , y , and z degrees of freedom, i.e., every element of the Green function becomes a 3×3 matrix. An example of this type of calculation can be found in Ref. [26]. The effect of finite system size of thermal fluctuations has been studied for three-dimensional systems using numerical simulations [27]. These investigations agree qualitatively with our results in one dimension, but show that, when extra dimensions are added and anharmonicity is taken into account, the lattice dynamics calculations may be significantly different from the molecular dynamics observations. Moreover, one could, in principle, even go beyond the approximation of rigid substrates and take into account the vibrations of the substrate atoms [25].

VII. CONCLUSION

In this work we have used molecular dynamics to investigate the melting of a thin confined film. Such calculations must always be taken with caution because their validity relies on the validity of the model itself. However, we think that one can draw some conclusions with a reasonable confidence for two reasons: (1) some of our conclusions are well corroborated by the experiments and (2) the physics lying behind the main results relies on simple arguments, related to the influence of the substrate on the structure and dynamics of the film.

One result that emerges from the simulations is that, for such a highly confined medium, the distinction between the solid and liquid phases is not as strict as for a bulk material. It cannot be simply established on considerations based on the structural organization and mobility of the atoms. Instead, the liquid can be characterized by the property that it does not sustain a shear stress, while the solid does. The liquid phase retains a significant degree of layering and this has previously been noticed by various authors, both from experimental or from numerical studies [1–3]. The solid shows a large degree of dynamical disorder. This is an aspect that has only been recently noticed in the experiments because in order to detect this phenomenon it is not sufficient to measure a global quantity such as the force acting on the whole sample in a surface force apparatus. One must be able to follow the molecular displacement in a microscopic regions. Fluorescence correlation spectroscopy has observed

this phenomenon [4]. Molecular dynamics calculations are very complementary of such experiments because they allow a detailed observation of the dynamics of the atoms in the confined solid, and, in particular, they can observe the anisotropy of the diffusion associated to the confinement. Moreover, while experiments may suffer from the difficulty to prepare very clean confining surfaces and to characterize them [21], simulations allow studies on perfectly controlled systems. The possibility to determine the equilibrium structure of the confined film suggests the following explanation for the high atomic mobility in the solid phase. The influence of the substrate, which is incommensurate with the solid lubricant as one can expect in most cases, distorts the solid structure of the lubricant. This distortion tends to stay rather localized in some regions, under the form of discommensurations, which leave some vacant spaces that make atomic diffusion easier.

The simulations have allowed us to observe the thermally induced melting. For very narrow layers, it appears to be associated to the formation of one additional layer in the lubricant. In their experimental studies of confinement-induced liquid-to-solid transition Klein and Kumacheva [3] had also noticed a change in film thickness, which was consistent with a change of one unit in the number of layers. But the simulations have also allowed us to determine the variation of the melting temperature T_m as a function of the film thickness, contrary to previous numerical studies of confined film melting, which had been essentially concerned with friction and shear-induced melting. In agreement with experiments that show that highly confined materials can be found in the solid phase at temperatures well above their bulk melting temperatures [3], we find that the melting temperature decreases when the thickness of the film increases. The phenomenological theory that we have proposed is based on the Lindemann criterion of melting and it treats the dynamics of the confined lubricant at the microscopic scale. Although it uses only one adjustable parameter, the parameter β_L that measures the threshold of the fluctuations that lead to melting in the Lindemann picture, it provides a good agreement with the molecular dynamics results. Moreover, one can notice that the value that we obtain for β_L is within the fairly narrow range generally that characterizes the Lindemann criterion.

ACKNOWLEDGMENTS

This research was supported in part by the NATO Grant No. HTECH.LG.971372 and the EU Contract No. HPRN-CT-1999-00163 (LOCNET network).

-
- [1] B.N.J. Persson, *Sliding Friction: Physical Principles and Applications* (Springer-Verlag, Berlin, 1998); Surf. Sci. Rep. **33**, 83 (1999).
 [2] M.O. Robbins and M.H. Müser, in *Handbook of Modern Tribology*, edited by B. Bhushan (CRC Press, Boca Raton, FL, 2000).
 [3] J. Klein and E. Kumacheva, Science **269**, 816 (1995); J. Chem.

Phys. **108**, 6996 (1998); E. Kumacheva and J. Klein, *ibid.* **108**, 7010 (1998).

- [4] A. Mukhopadhyay, J. Zhao, S.C. Bae, and S. Granick, Phys. Rev. Lett. **89**, 136103 (2002).
 [5] F.F. Abraham, J. Chem. Phys. **68**, 3713 (1978).
 [6] S. Toxvaerd, J. Chem. Phys. **74**, 1998 (1981).
 [7] R.G. Horn and J.N. Israelachvili, J. Chem. Phys. **75**, 1400

- (1981).
- [8] M. Plischke and D. Henderson, *J. Chem. Phys.* **84**, 2846 (1986).
- [9] P.A. Thompson and M.O. Robbins, *Science* **250**, 792 (1990); M.O. Robbins and P.A. Thompson, *ibid.* **253**, 916 (1991).
- [10] P.A. Thompson, M.O. Robbins, and G.S. Grest, *Isr. J. Chem.* **35**, 93 (1995).
- [11] A.V. Tkachenko and Y. Rabin, *Solid State Commun.* **103**, 361 (1997).
- [12] A. Weinstein and S.A. Safran, *Europhys. Lett.* **42**, 61 (1998).
- [13] O.M. Braun and M. Peyrard, *Phys. Rev. E* **63**, 046110 (2001).
- [14] P.A. Thompson and M.O. Robbins, *Phys. Rev. A* **41**, 6830 (1990).
- [15] M. Schoen, C.L. Rhykerd, D.J. Diestler, and J.H. Cushman, *Science* **245**, 1223 (1989).
- [16] J. Gao, W.D. Luedtke, and U. Landman, *J. Chem. Phys.* **106**, 4309 (1997).
- [17] J. Gao, W.D. Luedtke, and U. Landman, *J. Phys. Chem. B* **101**, 4013 (1997).
- [18] J.-P. Hansen and L. Verlet, *Phys. Rev.* **184**, 151 (1969).
- [19] M.H. Müser and M.O. Robbins, *Phys. Rev. B* **61**, 2335 (2000).
- [20] J.E. Curry, F. Zhang, J.H. Cushman, M. Schoen, and D. Diestler, *J. Chem. Phys.* **101**, 10 824 (1994).
- [21] M. Heuberger and M. Zäch, *Langmuir* **19**, 1943 (2003).
- [22] Ph. Valadon, RasTop: molecular visualization software, version 1.3.1 (<http://www.geneinfinity.org/rastop/>).
- [23] A.R. Ubbelohde, *The Molten State of Matter: Melting and Crystal Structure* (Wiley, Chichester, 1978), and references therein.
- [24] M. Kosevich, *Fundamentals of Crystal Lattice Mechanics* (Nauka, Moscow, 1972).
- [25] O.M. Braun, *Surf. Sci.* **213**, 336 (1989).
- [26] O.M. Braun, T. Dauxois, and M. Peyrard, *Phys. Rev. B* **56**, 4987 (1997).
- [27] M.O. Robbins, G.S. Grest, and K. Kremer, *Phys. Rev. B* **42**, 5579 (1990).